

Stimuli-Triggered Multishape, Multimode, and Multistep Deformations Designed by Microfluidic 3D Droplet Printing

Chenjing Yang, Yao Xiao, Lingjie Hu, Jingyi Chen, Chun-Xia Zhao, Peng Zhao, Jian Ruan, Ziliang Wu, Haifeng Yu, David A Weitz, and Dong Chen*

Elastomers generally possess low Young's modulus and high failure strain, which are widely used in soft robots and intelligent actuators. However, elastomers generally lack diverse functionalities, such as stimulated shape morphing, and a general strategy to implement these functionalities into elastomers is still challenging. Here, a microfluidic 3D droplet printing platform is developed to design composite elastomers architected with arrays of functional droplets. Functional droplets with controlled size, composition, position, and pattern are designed and implemented in the composite elastomers, imparting functional performances to the systems. The composited elastomers are sensitive to stimuli, such as solvent, temperature, and light, and are able to demonstrate multishape (bow- and S-shaped), multimode (gradual and sudden), and multistep (one- and two-step) deformations. Based on the unique properties of droplet-embedded composite elastomers, a variety of stimuli-responsive systems are developed, including designable numbers, biomimetic flowers, and soft robots, and a series of functional performances are achieved, presenting a facile platform to impart diverse functionalities into composite elastomers by microfluidic 3D droplet printing.

1. Introduction

Soft materials, such as polymers, hydrogels, and elastomers, are deformable under external stresses, and show broad applications in wearable devices, soft robots, and intelligent

actuators.[1-4] Among these soft materials, elastomers, which own low Young's modulus and high failure strain, demonstrate superior advantages to mimic natural systems.[5-7] For example, silicone elastomer, a typical viscoelastic elastomer, has unique hydrophobicity, good permeability for organic solvents (e.g., ethanol and methanol),[8,9] low permeability for water, and good processability. However, elastomers by themselves generally lack diverse functionalities, such as biomimetic performances and stimuli-triggered responses, severely limiting their applications.[10,11] Therefore, a lot of studies are committed to the development of composite elastomers with specific functionalities and performances.[12-14]

Generally, functional inclusions, such as droplets, bubbles, or particles,[15-19] are implemented into composite elastomers to endow the systems with superior performances, such as large actuation

capability,[20,21] high electrical conductivity,[22-24] and good mechanical property.[25-27] Therefore, composite elastomers derive their unique properties and functionalities from both elastomer matrix and functional inclusions.[28,29] For example, droplets of liquid metals are dispersed in the elastic matrix to

C. Yang, P. Zhao, J. Ruan, D. Chen Department of Medical Oncology The First Affiliated Hospital School of Medicine Zhejiang University Hangzhou, Zhejiang Province 310003, P. R. China E-mail: chen_dong@zju.edu.cn C. Yang, Y. Xiao, L. Hu, J. Chen, D. Chen Zhejiang Key Laboratory of Smart Biomaterials College of Chemical and Biological Engineering Zhejiang University Hangzhou, Zhejiang Province 310027, P. R. China C. Yang, D. Chen College of Energy Engineering and State Key Laboratory of Clean Energy Utilization **Zhejiang University** Hangzhou, Zhejiang Province 310003, P. R. China

The ORCID identification number(s) for the author(s) of this article

can be found under https://doi.org/10.1002/smll.202207073.

I. Chen. D. A. Weitz John A. Paulson School of Engineering and Applied Sciences Harvard University Cambridge, MA 02138, USA School of Chemical Engineering and Advanced Materials The University of Adelaide Adelaide, SA 5005, Australia Department of Polymer Science and Engineering **Zhejiang University** Hangzhou, Zhejiang Province 310003, P. R. China Department of Materials Science and Engineering **Peking University**

DOI: 10.1002/smll.202207073

Beijing 100871, P. R. China

1613629, 0, Downloaded from https://onlinelibrary.wiley.com/doi/10.1002/sml1.202207073 by Harvard University, Wiley Online Library on [31/01)2023]. See the Terms and Conditions (https://onlinelibrary.wiley.com/eran-and-conditions) on Wiley Online Library for rules of use; OA articles are governed by the applicable Creative Commons Licensean Conditions (https://onlinelibrary.wiley.com/eran-and-conditions) on Wiley Online Library for rules of use; OA articles are governed by the applicable Creative Commons Licensean Conditions (https://onlinelibrary.wiley.com/eran-and-conditions) on Wiley Online Library for rules of use; OA articles are governed by the applicable Creative Commons Licensean Conditions (https://onlinelibrary.wiley.com/eran-and-conditions) on Wiley Online Library for rules of use; OA articles are governed by the applicable Creative Commons Licensean Conditions (https://onlinelibrary.wiley.com/eran-and-conditions) on Wiley Online Library for rules of use; OA articles are governed by the applicable Creative Commons Licensean Conditions (https://onlinelibrary.wiley.com/eran-and-conditions) on Wiley Online Library for rules of use; OA articles are governed by the applicable Creative Commons Licensean Conditions (https://onlinelibrary.wiley.com/eran-and-conditions) on Wiley Online Library for rules of use; OA articles are governed by the applicable Creative Commons (https://onlinelibrary.wiley.com/eran-and-conditions) on Wiley Online Library for rules of use; OA articles are governed by the applicable Creative Commons (https://onlinelibrary.wiley.com/eran-and-conditions) on Wiley Online Library for rules of use; OA articles are governed by the applicable Creative Commons (https://onlinelibrary.wiley.com/eran-and-conditions) on Wiley Online Library for rules of use; OA articles are governed by the applicable Creative Commons (https://onlinelibrary.wiley.com/eran-and-conditions) on the applicable Creative Commons (https://onlinelibrary.wiley.com/eran-and-conditions) on the applicable Creative Commons (http

www.advancedsciencenews.com

www.small-journal.com

tailor the thermal and electrical conductivity of electric actuators.^[17,30] Currently, the implementation of functional droplets in composite elastomers generally relies on shearing to disperse them in the elastomer matrix, which lacks control over the size of functional droplets and their spatial distribution,^[31–33] thus limiting the design of dedicated and complicated systems.

To better design the composition, structure, and function of composite elastomers, a lot of efforts have been dedicated to implement functional droplets in an ordered way, [34-37] and different strategies are developed for the rapid prototyping of composite elastomers. [38-40] For example, microfluidic-based technologies are developed to construct composite elastomers with 3D architectures, whose local composition and property can be programmably tailored. [41,42] Despite of all the advances, it is still challenging to implement functional droplets in the composite elastomers with precisely controlled size, composition, position, and pattern. Innovations of novel strategies and technologies are required for the facile design of composite elastomers with desired functionalities.

Here, a facile microfluidic 3D droplet printing platform is developed to design stimuli-triggered multishape, multimode, and multistep deformations in composite elastomers. Silicone elastomer is chosen as the elastic matrix and arrays of micronsized functional droplets with precisely controlled size, composition, position, and pattern are embedded in the matrix. Designed composite elastomers possess diverse functionalities and superior performances, showing stimuli-triggered multishape, multimode, and multistep deformations. Various intelligent systems are designed based on the composite elastomers, including designable numbers, biomimetic flowers, and soft robots. The superior performances demonstrated by the composite elastomers suggest that microfluidic 3D droplet printing is a facile platform for the design of composite elastomers with controllable deformations and diverse functionalities.

2. Results and Discussions

To prepare functional composite elastomers, a facile platform of microfluidic 3D droplet printing is developed to print functional droplets in the elastomer matrix, as modeled in Figure 1 and demonstrated in Movies S1 and S2 (Supporting Information). The position of the printer head and the infusion of the syringe pump are precisely controlled by the system via programmable codes; functional droplets are then extruded into the 3D elastomer matrix at predesigned positions. After extrusion, functional droplets are detached from the nozzle under the viscous drag of the elastomer matrix as the nozzle rises. The microfluidic 3D droplet printing system combines the advantages of microfluidics and 3D printing, and the versatile platform allows the implementation and patterning of diverse functional droplets in the elastomer matrix, thus enabling the design of multi-shape (bow- and S-shaped), multi-mode (gradual and sudden), and multi-step (one- and two-step) deformations, as schematically shown in Figure 1. Due to the diverse characteristics of functional droplets, the deformations could be triggered by various stimuli of different mechanisms, such as solvent-triggered droplet swelling, temperature-triggered solvent vaporization, and light-triggered phase transition.

To demonstrate the flexible design of diverse composite elastomers via microfluidic 3D droplet printing, water droplets are used as model functional droplets. To avoid the drifting of printed droplets under buoyancy or gravity (Figure S1, Supporting Information), the density of water droplets is matched with that of the elastomer matrix ($\rho \approx 1.036$ g cm⁻³) by tuning the concentration of NaCl in water, as shown in Figure S2 (Supporting Information). When printed droplets are off the center of composite elastomers, e.g., near the top surface, and the elastomers are submerged in an organic solvent, which could diffuse across the elastomer and freely mix with water, e.g., methanol or ethanol, water droplets are swollen by the organic solvent due to osmotic pressure and their swelling thus results in the asymmetric bending of the elastomer strip toward its bottom, as illustrated in Figure 2a and Figure S3 (Supporting Information). Generally, both the swelling volume of water droplets and the bending amplitude of bow-shaped elastomers increase over the swelling time, as shown in Figure 2b.

In addition to swelling time, other parameters, such as the radius of water droplets, r, the distance between neighboring droplets, D, and the height between water droplets and elastomer surface, H, will affect the shape and amplitude of deformations, as shown in Figure 2a. Generally, the bulge angle and amplitude of the elastomer surface are caused by droplet swelling and they increase as the original droplet radius and swelling time increase, as shown in Figure 2c,d and Figure S4 (Supporting Information). Since the bending of elastomer strips is caused by the swelling of functional droplets, the bending angle of elastomer strips also increases as the original droplet radius and swelling time increase, as shown in Figure S5 (Supporting Information). Meanwhile, swelling of water droplets in ethanol over time and the induced bulge on the surface are inversely proportional to the neighboring droplet distance, as shown in Figure S6 (Supporting Information). In a typical composite elastomer, the radius of functional droplets is $r \approx 0.4$ mm, the distance between neighboring droplets is $D\approx 2$ mm, and the height between functional droplets and elastomer surface is $H\approx 0.2$ mm.

To better predict the shape and amplitude of the deformations, Finite Element Simulations are performed. The elastic strip is modeled as a hyperelastic material embedded with an array of uncompressible water droplets near the top surface. When the elastomer strip is submerged in methanol, water droplets swell, leading to the expansion of the strip top surface, and thus the curling toward its bottom surface, as simulated in Figure S7 (Supporting Information). Specifically, when the droplet radius increases from $r{\approx}0.5$ to 1.13 mm, the bending angle of the elastomer strip increases from 0° to 113° , which is consistent with the experimental results.

In additional to simple bow-shaped deformation, complex S-shaped deformation is designed by printing one array of water droplets near the top surface on the left of the elastomer strip and another array of water droplets near the bottom surface on the right of the strip, as shown in Figure 2e. Therefore, the left of the elastomer strip curves down while the right of the strip curves up, forming an S shape. Complex deformations could also be achieved by designing the shape of elastomer strips; upon droplet swelling, a cross-shaped elastomer strip will deform into a claw, as shown in Figure S8 (Supporting Information). The deformations caused by solvent-triggered

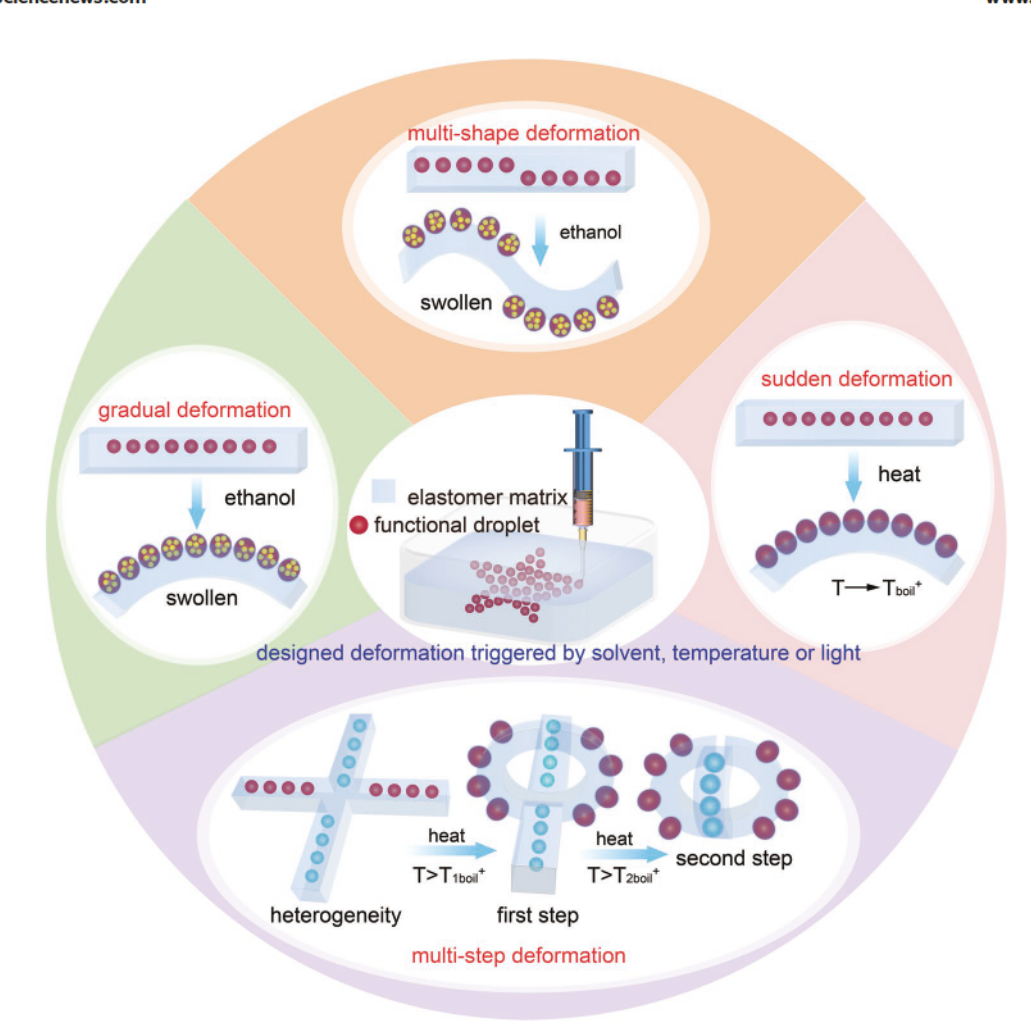


Figure 1. Multishape, multimode, and multistep deformations of composite elastomers designed by microfluidic 3D droplet printing and triggered by solvent, temperature, or light. A versatile platform of printing predesigned patterns of functional droplets in an elastomer matrix is developed to achieve multishape (bow- and S-shaped), multimode (gradual and sudden), and multistep (one- and two-step) deformations; these deformations could be triggered by various stimuli of different mechanisms, such as solvent-triggered droplet swelling, temperature-triggered solvent vaporization, and light-triggered phase transition.

droplet swelling are reversible. Swollen water droplets could be deswollen by submerging the elastomer strip in water, in which organic solvents will gradually diffuse out off the water droplets. Therefore, reversible deformation and recovery of the composite elastomers could be achieved by swelling water droplets in an organic solvent and deswelling water droplets in water, respectively.

While swelling liquid droplets in a solvent provide a strategy for gradual deformation, vaporization of liquid droplets above their boiling point could result in sudden deformation, as shown in Figure 2f. When the temperature is below the boiling point of water droplets, there is no observable deformation of the elastomer strip. Once the temperature increases above $T_{\rm boiling}$, water vaporizes and water droplets expand quickly, leading to the sudden curling of the elastomer strip in a couple of seconds, as shown in Figure S9 (Supporting Information). The elastomer strip will recover to its original shape in several minutes when the temperature is reduced below $T_{\rm boiling}$.

Multistep deformations of the composite elastomers could be achieved by printing functional droplets of different properties in different regions. For example, droplets of 71% water and 29% isopropanol with $T_{1boiling} \approx 89$ °C are printed in the horizontal strip of a cross-shaped strip, while water droplets with $T_{2\text{boiling}} \approx 100$ °C are printed in the vertical strip. When the composite elastomer is heated to $T\approx89$ °C ($T\geq T_{1boiling}$), droplets in the horizontal strip vaporize and expand, leading to the first-step curling of the horizontal strip, as shown in Figure 3a. When further heating the cross-shaped strip to T≈100 °C (T≥T_{2boiling}), droplets in the vertical strip vaporize and expand, causing the second-step deformation of the vertical strip. In addition to printing functional droplets of different properties in different regions, multistep deformations could also be achieved by utilizing the solid, liquid, and vapor states of functional droplets. When a straight elastomer strip is first stretched along its horizontal direction, spherical droplets are deformed into prolate shape, which are then fixed by freezing water droplets at -4 °C. After freezing, the stretching is removed and deformed prolate droplets lead to the extension of the strip top surface and thus the curling of the elastomer strip, as shown in Figure 3b. When the temperature increases

16136289, Q. Downloaded from https://onlinelibrary.wiley.com/doi/10.1002/sml1202207073 by Harvard University, Wiley Online Library on [31/012023]. See the Terms and Conditions (https://onlinelibrary.wiley.com/terms-and-conditions) on Wiley Online Library for rules of use; OA articles are governed by the applicable Creative Commons Licensens and Conditions (https://onlinelibrary.wiley.com/terms-and-conditions) on Wiley Online Library for rules of use; OA articles are governed by the applicable Creative Commons Licensens and Conditions (https://onlinelibrary.wiley.com/terms-and-conditions) on Wiley Online Library for rules of use; OA articles are governed by the applicable Creative Commons Licensens and Conditions (https://onlinelibrary.wiley.com/terms-and-conditions) on Wiley Online Library for rules of use; OA articles are governed by the applicable Creative Commons Licensens and Conditions (https://onlinelibrary.wiley.com/terms-and-conditions) on Wiley Online Library for rules of use; OA articles are governed by the applicable Creative Commons Licensens and Conditions (https://onlinelibrary.wiley.com/terms-and-conditions) on Wiley Online Library for rules of use; OA articles are governed by the applicable Creative Commons Licensens and Conditions (https://onlinelibrary.wiley.com/terms-and-conditions) on Wiley Online Library for rules of use; OA articles are governed by the applicable Creative Commons and Conditions (https://onlinelibrary.wiley.com/terms-and-conditions) on Wiley Online Library for rules of use; OA articles are governed by the applicable Creative Commons and Conditions (https://onlinelibrary.wiley.com/terms-and-conditions) on Wiley Online Library for rules of use; OA articles are governed by the applicable Creative Commons and Conditions (https://onlinelibrary.wiley.com/terms-and-conditions) on the applicable Creative Commons and Conditions (https://onlinelibrary.wiley.com/terms-and-conditions) on the applicable Creative Commons (https://onlinelibrary.wiley.com/terms-and-conditions) on the appli

www.advancedsciencenews.com

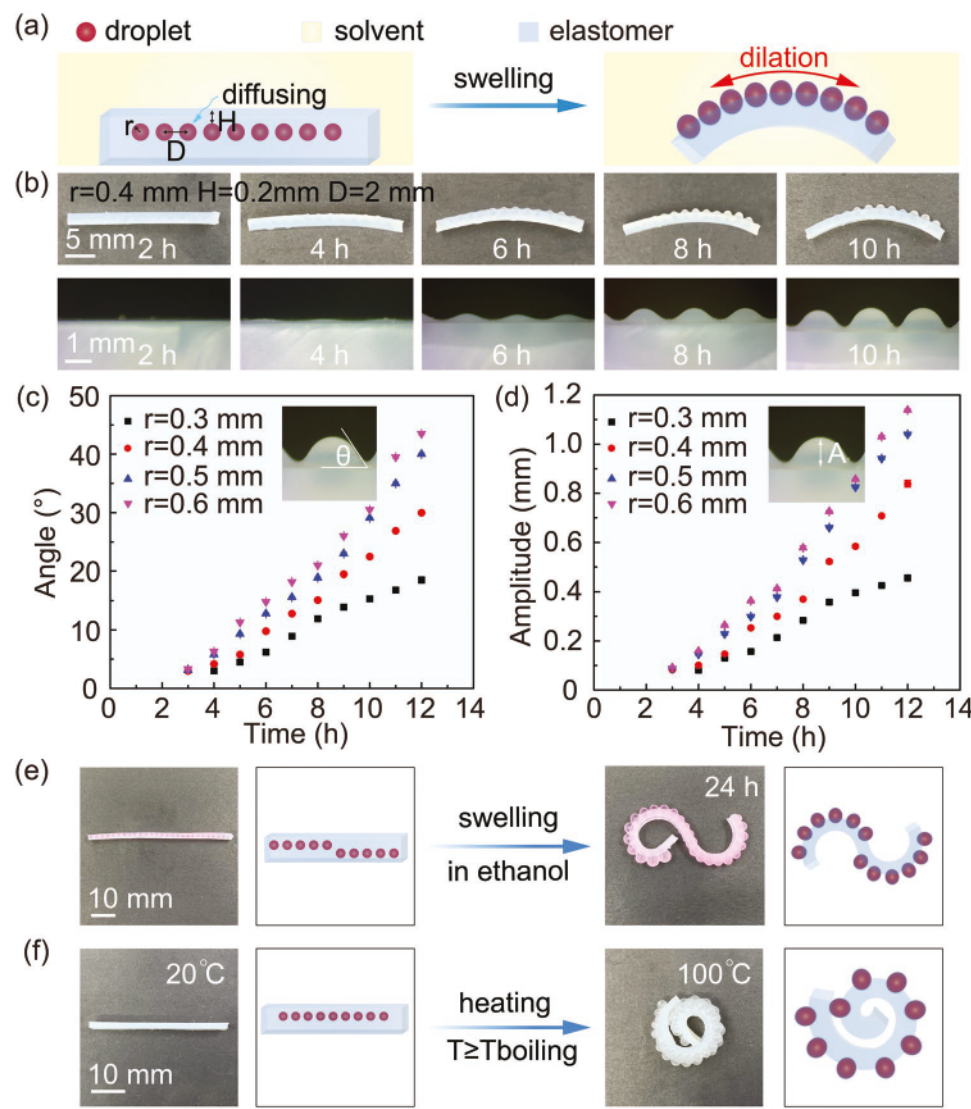


Figure 2. Gradual and sudden deformations of composite elastomers with controlled amplitude and shape. a) Schematics showing the swelling of water droplets in the elastomer matrix by ethanol and the induced deformation. b) Optical and microscope images showing the bulge size and bowshaped deformation caused by water droplet swelling in ethanol for different time. If not specified, the radius of water droplets is r≈0.4 mm, the distance between neighboring droplets is D=2 mm, and the height between water droplet and elastomer surface is H=0.2 mm. c) Bulge angle and d) bulge amplitude of the elastomer surface caused by droplet swelling for different time. e) S-shaped deformation designed by controlling the horizontal and vertical distributions of functional droplets. f) Sudden deformation achieved by temperature-triggered solvent vaporization ($T \ge T_{\text{boiling}}$).

to 20 °C, prolate ice droplets melt and recover back to spherical shape, accompanied by the first-step deformation of the elastomer strip back to its original straight shape. When further increasing the temperature to 100 °C, water droplets vaporize and expand, causing the second-step curling of the elastomer strip. Ideally, liquids, which are immiscible with the silicone elastomer matrix, could be printed in the elastomer matrix, which provides the flexibility in terms of materials and thus the tunability in terms of workable temperature range.

The composite elastomers possess many functionalities, including gradual deformation, sudden deformation, solventtriggered deformation, temperature-triggered deformation, multistep deformation, and multishape deformation, which provide a versatile platform for the design of various functional materials. For example, by controlling the horizontal and vertical distributions of functional droplets in a straight elastomer strip, a series of numbers, such as 6, 7, 8, and 9, are demonstrated when their deformations are triggered by solvent swelling, as shown in Figure 4a. Biomimetic system could also be designed by printing water droplets in the pedals of a flower, which shows reversible close-up and blossom when the system swells in ethanol and deswells in water, respectively, as shown in Figure 4b. Since the deformations could be designed and predicted by Finite Element Simulations (Figure S10, Supporting Information), soft robots are developed based on the composite elastomers, showing the encapsulation and release of a steel ball upon swelling in ethanol and deswelling in water, respectively, as shown in Figure 4c. The soft robot thus could grab an object and lift it up, as shown in Figure 4d.

16136269, 0, Downloaded from https://olinielibrary.wiley.com/doi/10.1002/sml1202207073 by Harvard University, Wiley Online Library on [31/012023]. See the Terms and Conditions (https://onlinelibrary.wiley.com/terms-and-conditions) on Wiley Online Library for rules of use; OA articles are governed by the applicable Creative Commons License

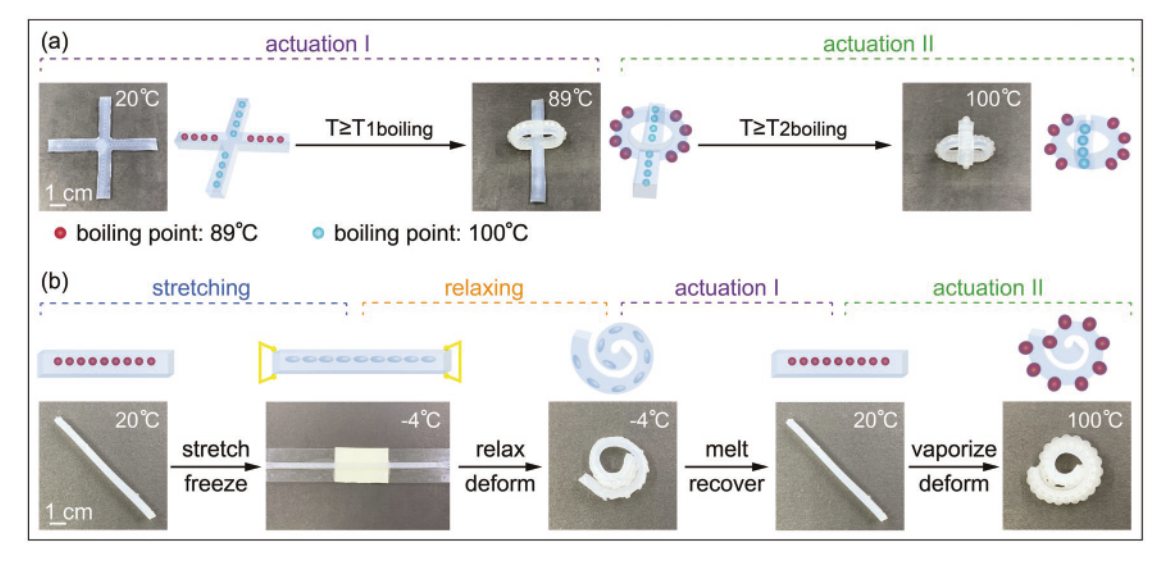


Figure 3. Multistep deformations of composite elastomers. a) Two-step deformations designed by using functional droplets with different boiling points. Functional droplets of 71% water and 29% isopropanol in the horizontal strip vaporize when T≥89 °C, leading to the first-step curling; upon further heating to T≥100 °C, water droplets in the vertical strip vaporize, resulting in the second-step deformation. b) Multistep deformations achieved by utilizing the solid, liquid, and vapor states of water droplets. The elastomer strip is first stretched along the horizontal direction to deform spherical water droplets into prolate shape. Prolate water droplets are frozen at -4 °C, and the elastomer strip automatically curls when the stretching is released. When the temperature increases above 0 °C, water droplets recover back to spherical shape, and the elastomer strip recovers to its original straight shape, showing the first-step deformation. The second-step deformation is achieved via the vaporization of water droplets at T≥100 °C.

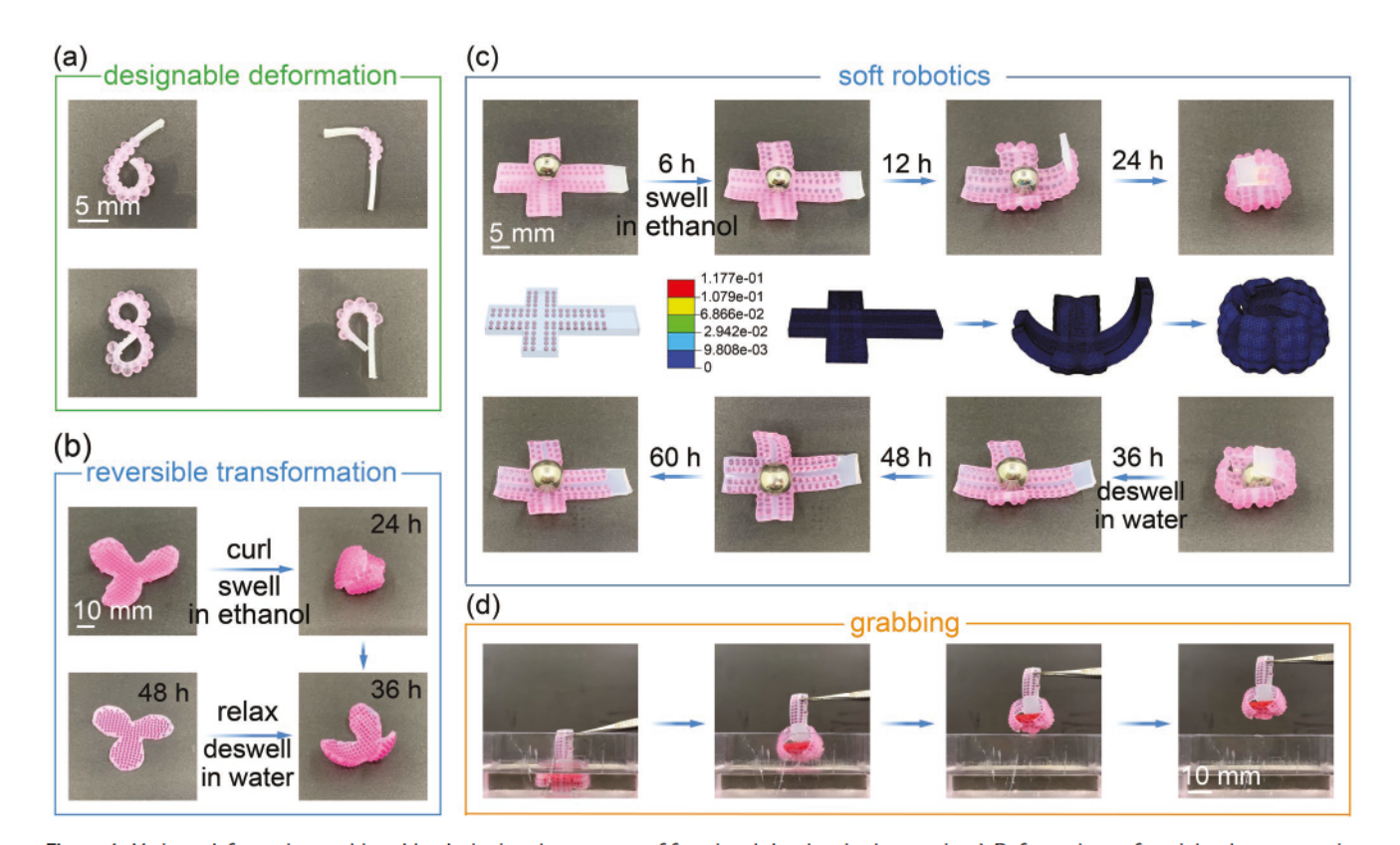


Figure 4. Various deformations achieved by designing the patterns of functional droplets in the matrix. a) Deformations of straight elastomer strips triggered by solvent swelling into different numbers of 6, 7, 8, and 9. Designable deformations are achieved by patterning functional droplets in the strip. b) Reversible close-up and blossom of a flower upon swelling in ethanol and deswelling in water, respectively. c) Encapsulation and release of a steel ball by the soft robot upon deformation and recovery, respectively. Finite element simulations predicting the deformations are consistent with the experimental results. d) Grabbing an object by the soft robot upon deformation.

www.advancedsciencenews.com

www.small-journal.com

16136289, Q. Downloaded from https://onlinelibrary.wiley.com/doi/10.1002/sml1202207073 by Harvard University, Wiley Online Library on [31/012023]. See the Terms and Conditions (https://onlinelibrary.wiley.com/terms-and-conditions) on Wiley Online Library for rules of use; OA articles are governed by the applicable Creative Commons Licensens and Conditions (https://onlinelibrary.wiley.com/terms-and-conditions) on Wiley Online Library for rules of use; OA articles are governed by the applicable Creative Commons Licensens and Conditions (https://onlinelibrary.wiley.com/terms-and-conditions) on Wiley Online Library for rules of use; OA articles are governed by the applicable Creative Commons Licensens and Conditions (https://onlinelibrary.wiley.com/terms-and-conditions) on Wiley Online Library for rules of use; OA articles are governed by the applicable Creative Commons Licensens and Conditions (https://onlinelibrary.wiley.com/terms-and-conditions) on Wiley Online Library for rules of use; OA articles are governed by the applicable Creative Commons Licensens and Conditions (https://onlinelibrary.wiley.com/terms-and-conditions) on Wiley Online Library for rules of use; OA articles are governed by the applicable Creative Commons Licensens and Conditions (https://onlinelibrary.wiley.com/terms-and-conditions) on Wiley Online Library for rules of use; OA articles are governed by the applicable Creative Commons and Conditions (https://onlinelibrary.wiley.com/terms-and-conditions) on Wiley Online Library for rules of use; OA articles are governed by the applicable Creative Commons and Conditions (https://onlinelibrary.wiley.com/terms-and-conditions) on Wiley Online Library for rules of use; OA articles are governed by the applicable Creative Commons and Conditions (https://onlinelibrary.wiley.com/terms-and-conditions) on the applicable Creative Commons and Conditions (https://onlinelibrary.wiley.com/terms-and-conditions) on the applicable Creative Commons (https://onlinelibrary.wiley.com/terms-and-conditions) on the appli

In the above studies, simple water droplets are used as the model functional droplets and the composite elastomers have demonstrated rich functionalities and diverse performances. The functionality of the composite elastomers could further be extended by diversifying the functionality of functional droplets. For example, to enable the remote manipulation of functional droplets between their solid and liquid states, azobenzene droplets are used as the functional droplets and programable deformations are achieved in a single composite elastomer. 4-Methoxyazobenzene is a typical photoresponsive material with an azobenzene group, which undergoes trans-cis and cistrans transformations upon exposure of UV and visible light, respectively, as shown in Figure 5a. Accompanying the transcis and cis-trans transformations, 4-methoxyazobenzene undergoes liquid-crystal and crystal-liquid transitions, respectively, since the UV-induced cis-configuration disorders the system and reduces the melting point of the system below room temperature. To demonstrate the programable deformations achievable in a single composite elastomer, an array of ordered azobenzene droplets are printed in a star-shaped elastomer. Different deformations are achieved via four steps, as shown in Figure 5b: (i) locally liquify azobenzene droplets in selected areas by remote patterning of UV light; (ii) stretch the composite elastomer to deform spherical droplets into prolate shape and solidify the deformed prolate droplets by visible light; (iii) after removing the stretching, deformed prolate droplets in selected areas maintain their shape and extend the elastomer along the stretching direction, thus leading to the deformation

of the composite elastomer into a predesigned shape; (iv) to recover the system, deformed prolate droplets are liquefied by UV exposure and the composite elastomer relaxes back to its original star shape. Therefore, by locally liquefying azobenzene droplets in selected areas via remote patterning of UV light, different deformations are achieved in a single elastomer, greatly facilitating the designing and engineering process.

3. Conclusion

Here, we develop a versatile platform to fabricate multifunctional composite elastomers embedded with droplet arrays via microfluidic 3D droplet printing. Compared with traditional 3D-printing techniques, such as fused deposition modeling, microfluidic 3D droplet printing is advantageous in designing smart and functional composite materials. The size, composition, and position of functional droplets in the elastomer matrix are precisely controlled by the platform, enabling the flexible design of stimuli-responsive systems, such as designable numbers, biomimetic flowers, and soft robots. Multishape (bow- and S-shaped), multi-mode (gradual and sudden), and multi-step (one- and two-step) reversible deformations are realized through the patterning of functional droplets in the composite elastomers and the deformations could be triggered by various stimuli of different mechanisms, such as solvent-triggered droplet swelling, temperature-triggered solvent vaporization, and light-triggered phase transition. The

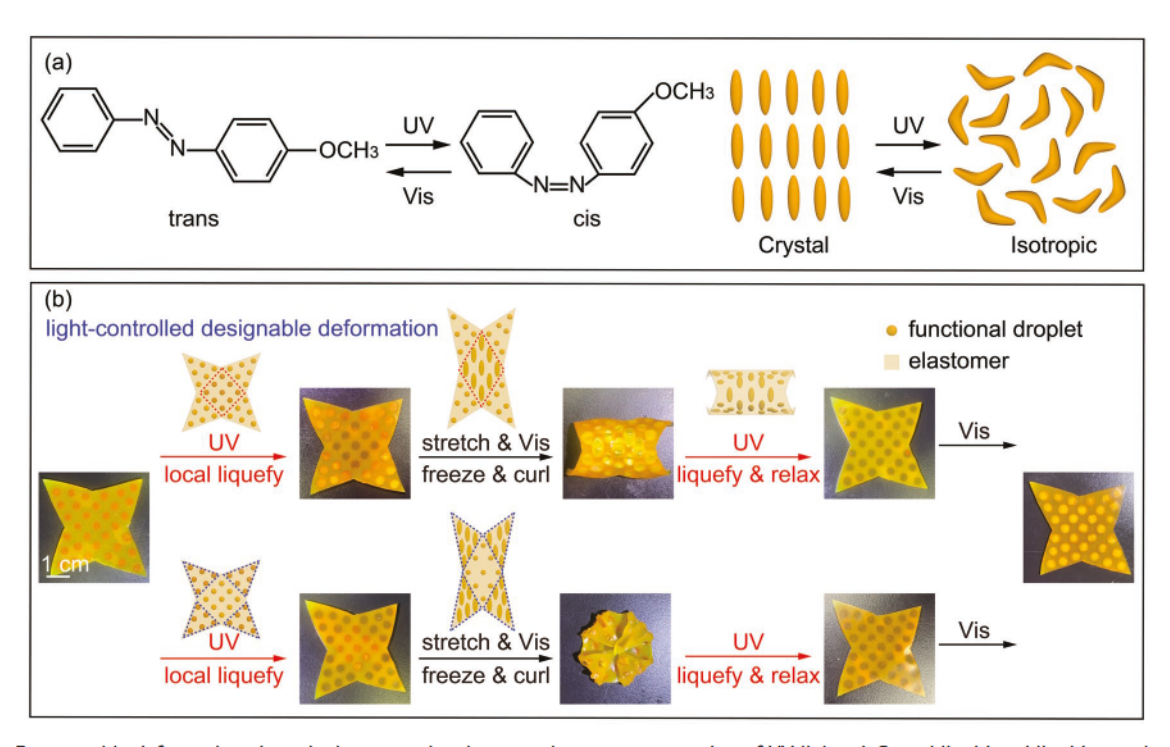


Figure 5. Programable deformations in a single composite elastomer by remote patterning of UV light. a) Crystal-liquid and liquid-crystal transitions of 4-methoxyazobenzene upon exposure of UV and visible light, respectively. b) Different deformations are achieved via four steps: i) locally liquify azobenzene droplets in selected areas (highlighted by dashed lines) by remote patterning of UV light; ii) stretch the composite elastomer to deform spherical droplets into prolate shape and solidify the deformed prolate droplets by visible light; iii) after removing the stretching, deformed prolate droplets in selected areas maintain their shape, leading to the deformation of the composite elastomer into a predesigned shape; iv) to recover the system, deformed prolate droplets are liquefied upon UV exposure and the composite elastomer relaxes back to its original shape.

www.advancedsciencenews.com

__ small

www.small-journal.com

properties of elastomers and the functionalities of droplets are well integrated in the composite elastomers by microfluidic 3D droplet printing, showing great potentials in designing and engineering materials with rich functionalities and diverse performances. Therefore, the microfluidic 3D droplet printing system is of great significance for smart and functional applications, especially in the interdisciplinary areas of soft matter, chemistry, biology, and robotics.

Supporting Information

Supporting Information is available from the Wiley Online Library or from the author.

Acknowledgements

This work is supported by the National Key Research and Development Program of China (grant No. YS2021YFC3000089), the Zhejiang Provincial Natural Science Foundation of China (grant No. Y20B060027), the National Natural Science Foundation of China (grant No. 22278352), the Zhejiang University Global Partnership Fund, ARC Discovery Project (grant Nos. DP200101238 and DP210103079), and NHMRC Investigator Grant (No. APP2008698). This work is also supported by the National Science Foundation of United States (grant No. DMR-1708729) and the National Science Foundation through the Harvard University MRSEC of United States (grant Nos. DMR-2011754 and DMR-1420570).

Conflict of Interest

The authors declare no conflict of interest.

Data Availability Statement

The data that support the findings of this study are available from the corresponding author upon reasonable request.

Keywords

3D printing, composite elastomers, functional droplets, microfluidics

Received: November 14, 2022 Revised: December 8, 2022 Published online:

- A. S. Gladman, E. A. Matsumoto, R. G. Nuzzo, L. Mahadevan, J. A. Lewis, *Nat. Mater.* 2016, 15, 413.
- [2] J. Chen, X. Liu, Y. Tian, W. Zhu, C. Yan, Y. Shi, L. B. Kong, H. J. Qi, K. Zhou, Adv. Mater. 2022, 34, 2102877.
- [3] Y. Zhao, Y. J. Tan, W. Yang, S. Ling, Z. Yang, J. T. Teo, H. H. See, D. K. H. Lee, D. Lu, S. Li, Adv. Healthcare Mater. 2021, 10, 2100221.
- [4] M. J. Han, D. K. Yoon, Engineering 2021, 7, 564.
- [5] Q. Ma, S. Liao, Y. Ma, Y. Chu, Y. Wang, Adv. Mater. 2021, 33, 2102096.
- [6] H. Shahsavan, S. M. Salili, A. Jákli, B. Zhao, Adv. Mater. 2015, 27, 6828.

- [7] C. Feng, C. P. H. Rajapaksha, A. Jákli, Engineering 2021, 7, 581.
- [8] H. T. Do Thi, P. Mizsey, A. J. Toth, Membranes 2020, 10, 345.
- [9] M. S. Javanmardi, E. Ameri, Polym. Bull. 2020, 77, 2591.
- [10] W. Feng, D. Liu, D. J. Broer, Small Struct. 2021, 2, 2000107.
- [11] J. Ma, Y. Yang, C. Valenzuela, X. Zhang, L. Wang, W. Feng, Angew. Chem., Int. Ed. 2022, 61, e202116219.
- [12] D. Rus, M. T. Tolley, Nature 2015, 521, 467.
- [13] C. Laschi, M. Cianchetti, Front. Bioeng. Biotechnol. 2014, 2, 1.
- [14] S. Kim, C. Laschi, B. Trimmer, Trends Biotechnol. 2013, 31, 287.
- [15] C. W. Visser, D. N. Amato, J. Mueller, J. A. Lewis, Adv. Mater. 2019, 31, 1904668.
- [16] B. M. Rauzan, A. Z. Nelson, S. E. Lehman, R. H. Ewoldt, R. G. Nuzzo, Adv. Funct. Mater. 2018, 28, 1707032.
- [17] M. J. Ford, C. P. Ambulo, T. A. Kent, E. J. Markvicka, C. Pan, J. Malen, T. H. Ware, C. Majidi, Proc. Natl. Acad. Sci. USA 2019, 116, 21438.
- [18] F. Ilievski, A. D. Mazzeo, R. F. Shepherd, X. Chen, G. M. Whitesides, Angew. Chem. 2011, 123, 1930.
- [19] L. Chen, C. Yang, Y. Xiao, X. Yan, L. Hu, M. Eggersdorfer, D. Chen, D. A. Weitz, F. Ye, *Mater. Today Nano* 2021, 16, 100136.
- [20] X. He, J. Wu, S. Xuan, S. Sun, X. Gong, ACS Appl. Mater. Interfaces 2022, 14, 9597.
- [21] S. Huang, Y. Huang, Q. Li, Small Struct. 2021, 2, 2100038.
- [22] E. J. Markvicka, M. D. Bartlett, X. Huang, C. Majidi, Nat. Mater. 2018, 17, 618.
- [23] L. Mou, J. Qi, L. Tang, R. Dong, Y. Xia, Y. Gao, X. Jiang, Small 2020, 16, 2005336.
- [24] Z. Feng, J. Guo, S. Liu, G. Feng, X.-H. Zhang, Chin. Chem. Lett. 2022, 33, 4021.
- [25] A. T. Haque, R. Tutika, R. L. Byrum, M. D. Bartlett, Adv. Funct. Mater. 2020, 30, 2000832.
- [26] Y. Jiang, Y. Wang, H. Wu, Y. Wang, R. Zhang, H. Olin, Y. Yang, Nano-Micro Lett. 2019, 11, 1.
- [27] Z. Wang, C. Valenzuela, J. Wu, Y. Chen, L. Wang, W. Feng, Small 2022, 18, 2201597.
- [28] S. I. Rich, R. J. Wood, C. Majidi, Nat. Electron. 2018, 1, 102.
- [29] C. Larson, B. Peele, S. Li, S. Robinson, M. Totaro, L. Beccai, B. Mazzolai, R. Shepherd, Science 2016, 351, 1071.
- [30] Z. Sun, C. Yang, M. Eggersdorfer, J. Cui, Y. Li, M. Hai, D. Chen, D. A. Weitz, Chin. Chem. Lett. 2020, 31, 249.
- [31] C. Yang, B. Wu, J. Ruan, P. Zhao, L. Chen, D. Chen, F. J. A. M. Ye, Adv. Mater. 2021, 33, 2006361.
- [32] C. Yang, B. Wu, J. Ruan, P. Zhao, J. Shan, R. Zhang, D. K. Yoon, D. Chen, K. Liu, ACS Appl. Polym. Mater. 2022, 4, 463.
- [33] A. Zhang, F. Wang, L. Chen, X. Wei, M. Xue, F. Yang, S. Jiang, Chin. Chem. Lett. 2021, 32, 2923.
- [34] C. P. Ambulo, J. J. Burroughs, J. M. Boothby, H. Kim, M. R. Shankar, T. H. Ware, ACS Appl. Mater. Interfaces 2017, 9, 37332.
- [35] H. J. Mea, L. Delgadillo, J. Wan, Proc. Natl. Acad. Sci. USA 2020, 117, 14700
- [36] A. Z. Nelson, B. Kundukad, W. K. Wong, S. A. Khan, P. S. Doyle, Proc. Natl. Acad. Sci. USA 2020, 117, 5671.
- [37] C. Yang, D. Chen, Chinese J. Liq. Cryst. Disp. 2022, 37, 1070.
- [38] R. L. Truby, J. A. Lewis, Nature 2016, 540, 371.
- [39] K. Hajash, B. Sparrman, C. Guberan, J. Laucks, S. Tibbits, 3D Print Addit. Manuf. 2017, 4, 123.
- [40] T. V. Neumann, M. D. Dickey, Adv. Mater. Technol. 2020, 5, 2000070.
- [41] T. J. Ober, D. Foresti, J. A. Lewis, Proc. Natl. Acad. Sci. USA 2015, 112, 12293.
- [42] B. Wu, C. Yang, Q. Xin, L. Kong, M. Eggersdorfer, J. Ruan, P. Zhao, J. Shan, K. Liu, D. Chen, D. A. Weitz, X. Gao, Adv. Mater. 2021, 33, 2102362